



Article

Bi₂Te₃ Thin Films Deposited by the Combination of Bi and Te Plasmas in a PLD Process

Laura A. Reyes-Verdugo ¹, C. D. Gutiérrez-Lazos ¹, J. Santos-Cruz ², A. Chávez-Chávez ³
and J. G. Quiñones-Galván ^{3,*}

¹ Centro de Investigación en Ciencias Físico Matemáticas, Facultad de Ciencias Físico Matemáticas, Universidad Autónoma de Nuevo León, Av. Universidad s/n. Ciudad Universitaria, San Nicolás de los Garza 66455, Mexico

² Facultad de Química, Materiales-Energía, Universidad Autónoma de Querétaro, Querétaro 76010, Mexico

³ Departamento de Física, Centro Universitario de Ciencias Exactas e Ingenierías, Universidad de Guadalajara, Boulevard Marcelino García Barragán 1421, Guadalajara 44430, Mexico

* Correspondence: jose.quinones@academicos.udg.mx

Abstract: Bismuth telluride thin films were grown by pulsed laser deposition by implementing a novel method that combines both Te and Bi plasmas resulting from the laser ablation of individual Bi and Te targets. Furthermore, the mean kinetic ion energy and density of the plasmas, as estimated by TOF curves obtained from Langmuir probe measurements, were used as control parameters for the deposition process. The obtained thin films exhibit a metallic mirror-like appearance and present good adhesion to the substrate. Morphology of the thin films was observed by SEM, yielding smooth surfaces where particulates were also observed (splashing). Chemical composition analysis obtained by EDS showed that apparently the films have a Te-rich composition (ratio of Te/Bi of 3); however, Te excess arises from the splashing as revealed by the structural characterization (XRD and Raman spectroscopy). The XRD pattern indicated that depositions have the rhombohedral (D_{3d}^5 ($R\bar{3}m$)) structure of Bi₂Te₃. Likewise, Raman spectra exhibited the presence of signals that correspond to E_g^2 , A_{1u}^2 and A_{1g}^2 (LO) vibrational modes of the same rhombohedral phase of Bi₂Te₃. Additionally, oxidation states, analyzed by XPS, resulted in signals associated to Bi³⁺ and Te²⁻ that correspond to the Bi₂Te₃ compound. Finally, surface topology and thickness profiles were obtained from AFM measurements, confirming a combination of a smooth surface with particulates on top of it and a film thickness of 400 nm.

Keywords: thin films; pulsed laser deposition; plasma parameters; bismuth telluride



Citation: Reyes-Verdugo, L.A.; Gutiérrez-Lazos, C.D.; Santos-Cruz, J.; Chávez-Chávez, A.; Quiñones-Galván, J.G. Bi₂Te₃ Thin Films Deposited by the Combination of Bi and Te Plasmas in a PLD Process. *Micromachines* **2023**, *14*, 590. <https://doi.org/10.3390/mi14030590>

Academic Editor: Aiqun Liu

Received: 1 February 2023

Revised: 24 February 2023

Accepted: 25 February 2023

Published: 28 February 2023



Copyright: © 2023 by the authors. Licensee MDPI, Basel, Switzerland. This article is an open access article distributed under the terms and conditions of the Creative Commons Attribution (CC BY) license (<https://creativecommons.org/licenses/by/4.0/>).

1. Introduction

Bismuth telluride (Bi₂Te₃) is a semiconductor material with a bandgap energy that varies in the range of 0.15 to 0.2 eV [1,2]. The crystal structure (rhombohedral), belonging to D_{3d}^5 ($R\bar{3}m$) space group, has an atomic arrangement based on Te⁽¹⁾–Bi–Te⁽²⁾–Bi–Te⁽¹⁾ layers, where the superscripts denote different states of the Te anions. This means that each neutral plane of Bi₂Te₃ structure is built by five monatomic planes bonded by covalent bonds along the C axis [1,3]. The Te–Bi bonds are polar, while the bonds between the Te⁽¹⁾–Te⁽¹⁾ planes are weaker than those of the polar type. Consequently, the two weakly bonded big ions, the telluride ions, will be highly polarizable, property that makes Bi₂Te₃ a widely studied material for photocatalytic and thermoelectric applications [4,5]. Therefore, the synthesis process for Bi₂Te₃, will highly influence its structure, morphology, chemical state, and size; properties that are of important interest in the above-mentioned technological areas.

Concerning the Bi₂Te₃ synthesis methods, the material was prepared successfully using techniques based on chemical reaction in solution, such as electroless deposition [6], electrochemical deposition [7], solvothermal [1], and sol–gel [8], among others. Such techniques require additional treatments to obtain a uniform and adherent thin film, free

of secondary phases formed by the employed chemical precursors. On the other hand, techniques based on physical vapor processes have also been successfully applied, among which we can mention the evaporation techniques such as pulsed laser deposition (PLD), lithography, spray pyrolysis, among others. The PLD technique, based on the laser ablation of solids, is a top-down method that takes advantage of the high energy of a pulsed laser to evaporate practically any type of materials, which allows its application in a great variety of fields. We can summarize the process of pulsed laser deposition of thin films in three stages, the assembly of ions, clusters and particles generated by the ablation process, nucleation, and growth.

Specifically, the laser ablation consists in the remotion of material from the surface of a solid by the application of short duration laser pulses of the order from 10^{-13} to 10^{-8} s, and power densities from 10^6 to 10^{14} W/cm² on the surface of the ablated target [9]. The removed material, also known as plasma plume, consists in a mixture of charged and neutral particles (electrons, ions, clusters, molecules, particulates) that will expand far from the surface and perpendicular to the ablated target. The ablation process can be carried out in vacuum, or in a gas or in a liquid environment, taking care that gas or liquid does not significantly attenuate energy or laser light intensity incident on the surface of the solid. This surrounding medium will determine the expansion and properties of the plasma. It is generally accepted that the resulting mean kinetic energies of the ions, within the interval of 1 to 300 eV, would allow the transport of material from the target to the substrate [10] to deposit a congruent thin film from compound targets. However, several considerations should take into account when preparing experiments regarding ablation of compound targets in order to diminish deviations in chemical composition of the targets and thin films. These considerations are highly dependent on the thermodynamic and optical absorption properties of the target. In some cases, loss of high volatile elements could be expected during the plasma expansion towards the target, making the congruent deposition a difficult task. To overcome this issue, plasma diagnosis has become a powerful tool that allows for shedding light on the mean kinetic energy and density of the arriving species on the substrate. Both parameters play an important role in the final composition, and thus properties of the growing films [11–13].

The electronic layer of the active plasma close to the surface substrate has a positive effect on the adhesion coefficient. The use of inert gas allows a reduction in the re-evaporation of volatile components of the films. An attractive aspect of this technique is its capacity for the tank of vapors at high pressures of reactive gases. This method has been used successfully to obtain thin Bi₂Te₃ films at temperatures around 300 °C [14].

To our knowledge, all works in literature reporting pulsed laser deposition of Bi₂Te₃ use a single compound target for the ablation process, which ends up in dealing with strategies to overcome deviations from the stoichiometry of the target in the final composition of the films along with elevated substrate temperatures or post-annealing treatments [14–19].

In the present work, bismuth telluride thin films were grown using PLD, combining both Te and Bi plasmas. Combination of plasmas to deposit compound or doped thin films controlling the chemical composition by means of plasma diagnosis tools has been previously reported in several works by our group [12,13,20–24]. The morphological, structural, chemical composition, and topological properties were studied for a fixed combination of Te/Bi ion density ratio.

2. Materials and Methods

Bismuth telluride thin films were grown using the pulsed laser deposition method. The deposition process was achieved by the combination of plasmas resulting from the simultaneous ablation of high purity Te and Bi targets. Figure 1a shows a schematic diagram of the PLD system. The Te target was obtained from the compression of high purity powders into a 1-inch pellet, while the Bi target was obtained from the melting of high purity Bi pellets in an inert atmosphere to avoid oxidation in a 1/2-inch pellet. Afterwards, the Bi pellet was attached coaxially to the Te target using double-sided carbon tape.

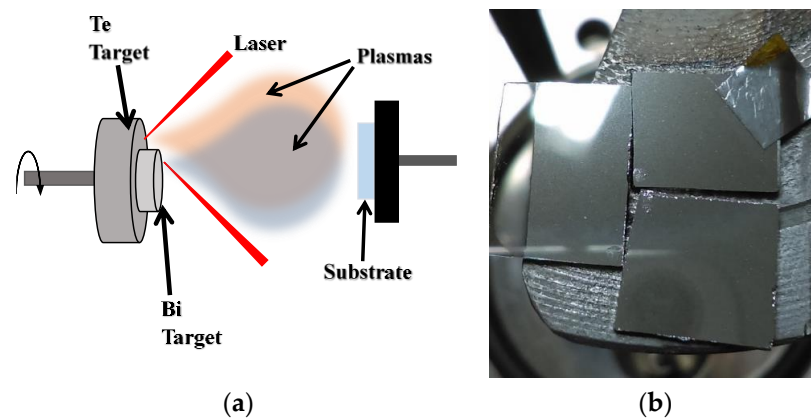


Figure 1. (a) PLD system configuration. (b) Deposited films.

For the laser ablation process a Nd:YAG laser emitting at 1064 nm with an output energy of 600 mJ per pulse, 6 ns duration pulses and repetition rate of 10 Hz, was used. The beam was divided into two equal beams using a 50–50 beam splitter. Each laser beam was focused on one of the targets while they were rotating at 15 rpm to avoid cumulative ablation in the same spot leading eventually to a drilling process. The target to substrate distance for Bi was 4.7 cm, while for Te it was 5 cm. The deposition chamber was evacuated to a base pressure of 3×10^{-6} Torr, which was also the working pressure. For the deposition process, glass slides were used as substrates keeping a deposition time of 20 min. Three substrates were used in a single experiment in order to evaluate uniformity of the films. The configuration of the substrates is shown in Figure 1b. On the right side of the substrate holder, two substrates with area of 1 cm^2 were placed, and at the left side a substrate of $1 \times 1.5 \text{ cm}^2$. Thickness of the films was measured at the corners of the substrates, and it was found that an approximate area of $(1.5 \times 1.5) \text{ cm}^2$ at the center of the array can be considered as uniform in thickness with a value of 400 nm. Regarding morphology, no substantial changes were observed. Additionally, due to the configuration of the targets, as it could be expected, the zones at the extremes sides of the array differed in chemical composition as one extreme was Bi rich while its counterpart was Te rich. In spite of the latter, at the center of the array, a uniform chemical composition was obtained. Regarding structural properties, the individual substrates were characterized, finding no substantial differences in the uniform observed zones.

Prior the deposition of the films, the individual Te and Bi plasmas were diagnosed by means of time of flight (TOF) measurements using a planar electrostatic Langmuir probe with 6 mm of diameter biased to -48 V , from which mean kinetic energy and ion density were obtained. For TOF measurements, the voltage drop across a 20 Ohm resistance was detected using a Tektronix 500 MHz digital oscilloscope. The calculation of mean kinetic energy of the ions uses the following relationship [25]:

$$\langle E_k \rangle = \frac{mL^2}{2} \frac{\int_0^T t^{-2} I(t) dt}{\int_0^T I(t) dt}$$

where m is the mass of the ion, L is the target to probe distance, and $I(t)$ is the probe current as a function of time. For the plasma ion density calculation, the following equation was used [20,26]:

$$N_p = \frac{I_{max}}{evA},$$

where I_{max} stands for the maximum value of the current (saturation current), e is the electron charge, v is the plasma flow velocity and A is the area of the probe. The obtained TOF curves with mean kinetic energy and density of Bi and Te ions is shown in Figure 2.

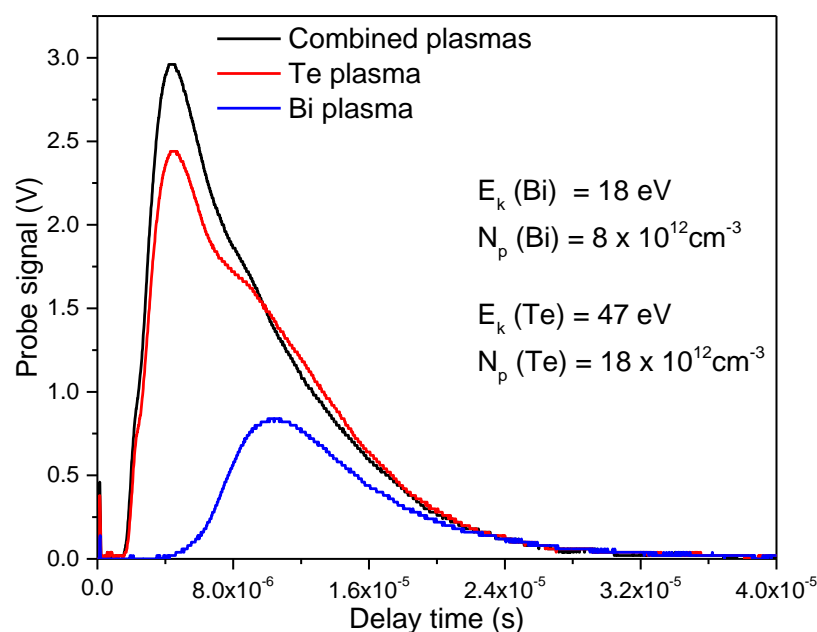


Figure 2. TOF curves for Bi and Te plasmas.

From Figure 2, it can be noticed that the plasma density ratio for Te and Bi was 2.25, which is higher than the Te/Bi ratio in Bi_2Te_3 . This higher ratio in the plasmas was chosen in order to compensate possible Te losses during the experiment aiming to obtain stoichiometric films. The use of individual Te and Bi targets to produce separated plasmas, that can be combined while expanding towards the substrate instead of a stoichiometric Bi_2Te_3 target, is preferred in this work, owing that required specific compositions can be more easily controlled by means of the plasma diagnosis tool. The fact of having separate individual beams impinging each target, allows manipulation of incident energy on the individual targets, which make that desired ion densities could be chosen searching for avoiding deviation from stoichiometry. In contrast, the use of stoichiometric targets would need several different experiments in order to find adequate conditions to obtain nearly stoichiometric films. Because Bi and Te have different vapor pressures, ablating with a single beam would necessarily induce Te losses that need to be compensated, or instead, avoided by the use of inert gases at higher pressures, compromising the deposition rate and structural properties of the films. Although it is accepted that laser ablation intrinsically produces congruent deposition of thin films from compound targets, this should be taken with care due it not being straightforward [25].

The surface morphology of the films was observed by scanning electron microscopy (SEM), using a JEOL JSM-6010LA microscope. Measurements were carried out at a 20 kV acceleration voltage. Chemical composition was studied by energy dispersive X-ray spectroscopy using an EDS detector attached to the SEM microscope. Structural characterization was carried out by X-ray diffraction using an empyrean system from PANALYTICAL (Malvern, UK) and Raman spectroscopy with a Thermo Scientific DXR2 system (Thermo Fisher Scientific Inc., Waltham, MA, USA) equipped with a 633 nm laser as excitation source. The oxidation states were studied using an X-ray photoelectron spectroscopy in a Flex-mod SPECS system (SPECS GmbH, Berlin, Germany) equipped with a PHOIBOS 100 detector. Surface topology and films thickness were measured by atomic force microscope using an Agilent Technologies system (Agilent Technologies, Inc., Santa Clara, CA, USA) model 5420 in contact mode.

3. Results and Discussion

3.1. Scanning Electron Microscopy

In Figure 3, a typical film surface micrograph from PLD of Bi and Te targets is shown. According to Dauscher et al. [15], different types of particulates may be observed when depositing Bi_2Te_3 with PLD, originating from target surface roughening as it has already been reported [27,28] and identified as defects produced due the laser irradiation (thermal and mechanical shocks). This is the well-known splashing phenomenon, one of the greatest disadvantages of the PLD technique. As discussed below, the EDS study confirms the presence of elemental Bi and Te at the surface of the films resulting from splashing of individual targets. Nevertheless, the surface of the films that is free from particulates appears to be dense and smooth.

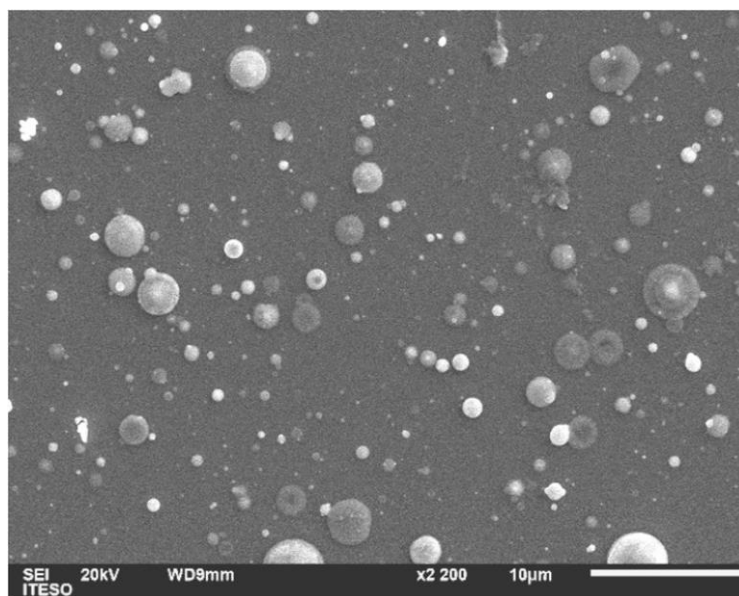


Figure 3. Scanning electron micrographs of Bi_2Te_3 film deposited by PLD technique.

3.2. EDS Analysis

Figure 4 shows a representative EDS spectrum for the Bi_2Te_3 film. Spectra for the films were recorded in different zones of the samples. Punctual measurements on individual particulates showed that they are composed either by a high percentage of Bi or Te. For the study presented here measurements of observed surfaces ($10 \times 10 \mu\text{m}^2$) were carried out at several regions of the samples; however, we present results corresponding to the central zone of the array shown in Figure 1b. Solely signals corresponding to Bi and Te are present, the atomic percentage for Bi and Te elements resulted in 25 and 75%, respectively, which correspond to a Te/Bi ratio of 3, which is considerably higher than the 2.25 ratio used in the plasma densities of Te and Bi. Considering a stoichiometric Bi_2Te_3 compound, atomic Te/Bi ratio should be 1.5; however, the apparent discrepancy between EDS composition results and stoichiometric Te/Bi ratio arises from the splashing mentioned above. Particulates of elemental Te and Bi contribute to the chemical composition determined by EDS. We see in the structural analysis and XPS results that the composition of film beneath the particulates is near to the desired stoichiometric compound.

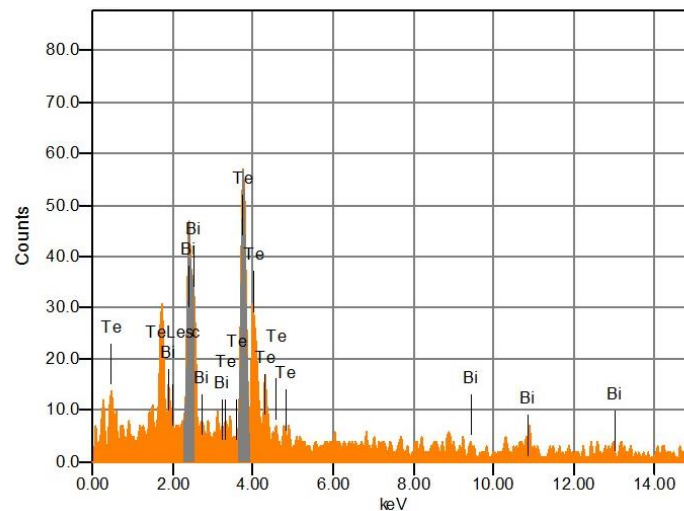


Figure 4. EDS spectrum of Bi_2Te_3 film deposited by PLD technique.

3.3. XRD Analysis

In Figure 5, the diffraction pattern obtained from a polycrystalline thin film deposited by the simultaneous ablation of Bi and Te targets is exhibited. The colored lines represent the reference standards for Bi_2Te_3 (red), Bi (green), and Te (blue) structures, according to the JCPDS-ICDD files 00-015-0863, 01-085-1329, and 00-036-1452, respectively. Depending on the film deposition technique, the intensity of the peaks may vary [27]; however, the preferred growth plane of all Bi_2Te_3 is shown at the (0 1 5) plane, around to 27.54° . A characteristic peak of films prepared by PLD is shown at the (0 0 6) plane, confirming that it is feasible to obtain at room temperature a film with a higher degree of crystallinity, in comparison with other deposition methods [29,30]. Note that the appearance of signals corresponding to elemental Bi and Te confirms the presence of splashing at the surface of the films, which is in accordance with SEM and EDS discussions. Crystallite size for Bi_2Te_3 was calculated using the Scherrer equation as ~ 55 nm, which is in good agreement with the Takashiri report [31], in which $\text{Bi}_2\text{Te}_{2.7}\text{S}_{0.3}$ was synthesized by means of the flash evaporation method. According to their discussion, nanocrystalline thin films based on bismuth telluride can potentially have improved thermoelectric responses due to quantum effects arising from size reduction. Therefore, obtaining small grain size (less than 200 nm) in bismuth telluride thin films is important for a possible application on thermoelectric devices with improved figure of merit [31–33]. Nevertheless, the present work is mainly focused on the synthesis method and the resulting structural, morphological, and chemical composition of the thin films.

3.4. Raman Analysis

A typical Raman spectrum of a synthesized Bi_2Te_3 thin film is shown in Figure 6. The presence of signals centered at 94, 120, and 139 cm^{-1} , assigned to the E_g^2 , A_{1u}^2 , and A_{1g}^2 (LO) vibrational modes, respectively, corresponding to the rhombohedral-structured Bi_2Te_3 , which are consistent with reports in the literature [31–34] and the XRD analysis.

As can be seen in Figure 6, mode E_g^2 is twofold degenerate in E_g^2 , which means that the atoms vibrate in the basal plane. On the other hand, notice that the A_{1u}^2 mode appears with the highest intensity in Figure 6. The appearance of A_{1u}^2 mode has been reported when crystal symmetry breaking occurs in nanoplates or nanosheets [1,2]; thus, it could be possible that bismuth telluride thin films of the present work are composed of thin structures stacked together to form crystallites with a 55 nm size.

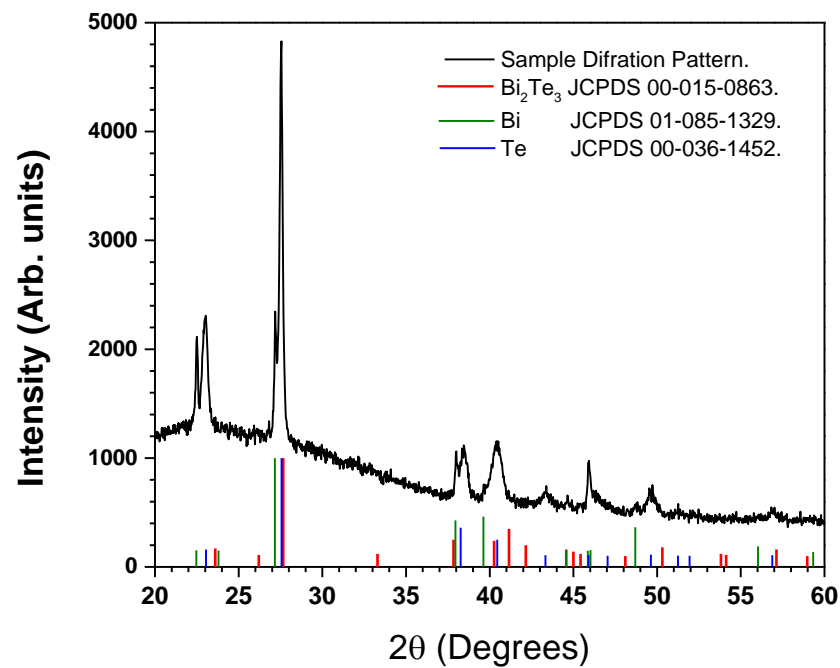


Figure 5. XRD Analysis of synthesized Bi_2Te_3 film.

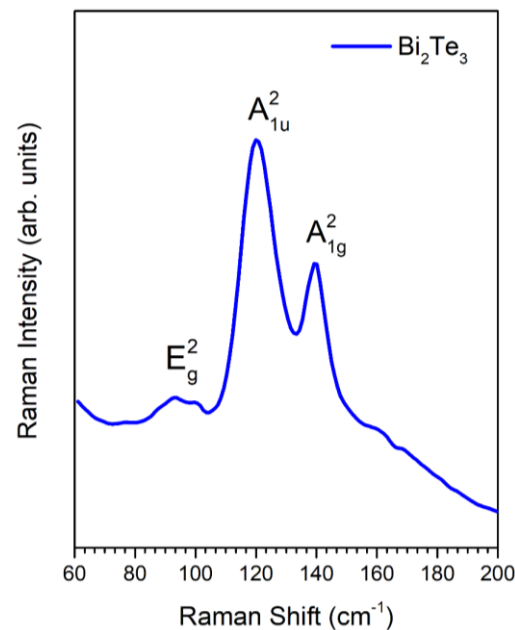


Figure 6. Raman spectrum of synthesized Bi_2Te_3 film.

3.5. XPS Analysis

Figure 7 shows the XPS spectra of the Bi_2Te_3 . The Te spectrum, Figure 6a, shows two sets of peaks at 570.82 and 580.94 eV, which correspond to $\text{Te}^{-2} 3d_{5/2}$ and $\text{Te}^{-2} 3d_{3/2}$. It also has small peaks at 573.88 and 584.11 eV due to surface oxidation. A previous study reported that nanostructured materials are more easily oxidized [35–37]. Figure 6b shows the high-resolution scan of Bi 4f doublet peaks centered at 155.78 eV and 161.10 eV, corresponding to $\text{Bi}^{+3} 4f_{7/2}$ and $\text{Bi}^{+3} 4f_{5/2}$, respectively, confirming the formation of the Bi_2Te_3 phase [37–40].

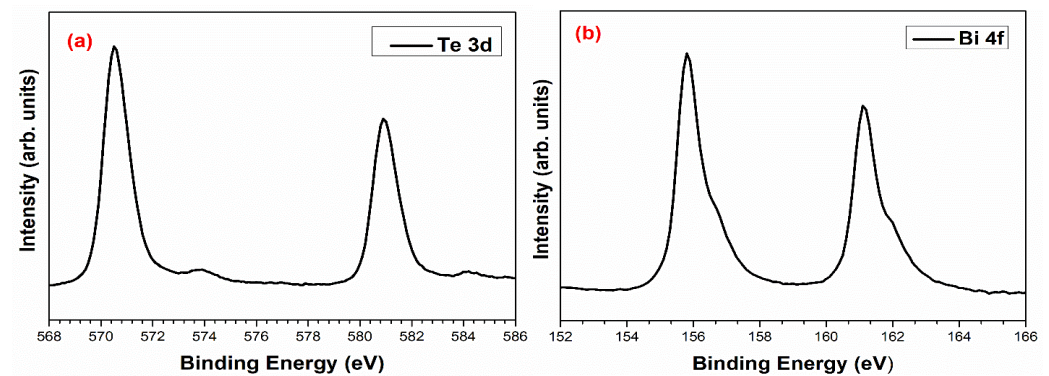


Figure 7. XPS spectra for (a) Te 3d and, (b) Bi 4f of synthesized Bi_2Te_3 thin film.

3.6. AFM Analysis

The thickness and surface topography of the films were determined using AFM measurements. Figure 8 shows an atomic force micrograph of the Bi_2Te_3 sample. Profile measurements at zone protected during the deposition to prevent material growth show that the thickness of the film is approximately 400 nm, which means that a deposition rate of 20 nm/min was achieved, which is important for thermoelectric applications.

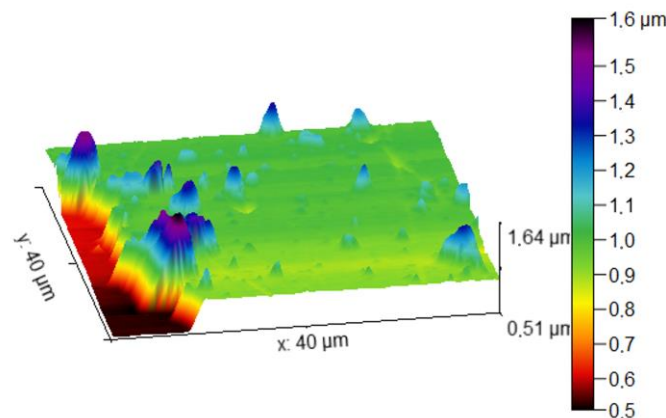


Figure 8. AFM micrograph for Bi_2Te_3 thin film.

The surface topology of the film shows that the areas that are free from splashing are dense and smooth, which is consistent with the SEM results. The presence of particulates can be seen through all the surfaces.

4. Conclusions

A simple way to elaborate bismuth telluride films by PLD with an innovative method using elemental Bi and Te Targets has been presented. Since there is a big difference between the bismuth and tellurium vapor pressures, obtaining satisfactory stoichiometry could be a challenge, but with convenient experimental conditions, it is feasible to achieve crystalline stoichiometric thin films even on substrates at room temperature. The XRD, EDS, and XPS results proved the crystallinity and chemical composition of the films, respectively. Raman studies confirmed the presence of Bi_2Te_3 characteristic vibrational modes. It can be concluded that the combination of laser-produced plasmas from the laser ablation of individual elemental targets demonstrated to be a powerful technique for the deposition of complex systems such as Bi_2Te_3 , for which applications are highly sensitive to elemental composition. Furthermore, the use of Langmuir planar probes for plasma diagnosis allows stoichiometry control as well as experimental reproducibility.

Author Contributions: L.A.R.-V. and J.G.Q.-G. wrote the main manuscript text; J.S.-C. contributed to Raman spectroscopy measurements and results interpretation; A.C.-C. contributed to XRD and SEM analysis and with funds for the research; C.D.G.-L. contributed to partial writing of the manuscript and XPS analysis. All authors have read and agreed to the published version of the manuscript.

Funding: This research was funded by Universidad de Guadalajara.

Data Availability Statement: The data presented in this study are available on request from the corresponding author.

Acknowledgments: The authors thank the technical support of Sergio Oliva, Ruben Montelongo, Ettore Vasallo and Juan Carlos Romero for their technical support.

Conflicts of Interest: The authors declare no conflict of interest.

References

1. Liang, Y.; Wang, W.; Zeng, B.; Zhang, G.; Huang, J.; Li, J.; Li, T.; Song, Y.; Zhang, X. Raman scattering investigation of Bi_2Te_3 hexagonal nanoplates prepared by a solvothermal process in the absence of NaOH. *J. Alloys Compd.* **2011**, *509*, 5147–5151. [\[CrossRef\]](#)
2. Kullmann, W.; Geurts, J.; Richter, W.; Lehner, N.; Rauh, H.; Steigenberger, U.; Eichhorn, G.; Geick, R. Effect of Hydrostatic and Uniaxial Pressure on Structural Properties and Raman Active Lattice Vibrations in Bi_2Te_3 . *Phys. Stat. Sol. B* **1984**, *125*, 131. [\[CrossRef\]](#)
3. Witting, I.T.; Chasapis, T.C.; Ricci, F.; Peters, M.; Heinz, N.A.; Hautier, G.; Snyder, G.J. The Thermoelectric Properties of Bismuth Telluride. *Adv. Electron. Mater.* **2019**, *5*, 1800904. [\[CrossRef\]](#)
4. Lee, S.; Esfarjani, K.; Luo, T.; Zhou, J.; Tian, Z.; Chen, G. Resonant bonding leads to low lattice thermal conductivity. *Nat. Commun.* **2014**, *5*, 3525. [\[CrossRef\]](#)
5. Zeier, W.G.; Zevalkink, A.; Gibbs, Z.M.; Hautier, G.; Kanatzidis, M.G.; Snyder, G.J. Thinking Like a Chemist: Intuition in Thermoelectric Materials. *Angew. Chem. Int. Ed.* **2016**, *55*, 6826. [\[CrossRef\]](#)
6. Scidone, L.; Diliberto, S.; Stein, N.; Boulanger, C.; Lecuire, J.M. Electroless method for Bi_2Te_3 film deposition. *Mat. Lett.* **2005**, *59*, 746–748. [\[CrossRef\]](#)
7. Kang, W.-S.; Chou, W.-C.; Li, W.-J.; Shen, T.-H.; Lin, C.-S. Electrodeposition of Bi_2Te_3 -based p and n-type ternary thermoelectric compounds in chloride baths. *Thin Solid Films* **2018**, *660*, 108–119. [\[CrossRef\]](#)
8. Zhao, Y.-J.; Zhou, F. Synthesis, Evolution of Morphology, Transport Properties for Bi_2Te_3 Nanoplates. *Crystals* **2022**, *12*, 1668. [\[CrossRef\]](#)
9. Yan, Z.; Chrisey, D.B. Pulsed laser ablation in liquid for micro-/nanostructure generation. *J. Photochem. Photobiol. C Photochem. Rev.* **2012**, *13*, 204–223. [\[CrossRef\]](#)
10. Lowndes, D.H.; Geohegan, D.B.; Poretzky, A.A.; Norton, D.P.; Rouleau, C.M. Synthesis of Novel Thin-Film Materials by Pulsed Laser Deposition. *Science* **1996**, *273*, 898. [\[CrossRef\]](#)
11. Wicklein, S.; Sambri, A.; Amoroso, S.; Wang, X.; Bruzzese, R.; Koehl, A.; Dittmann, R. Pulsed laser ablation of complex oxides: The role of congruent ablation and preferential scattering for the film stoichiometry. *Appl. Phys. Lett.* **2012**, *101*, 131601. [\[CrossRef\]](#)
12. Quiñones-Galván, J.G.; Lozada-Morales, R.; Jiménez-Sandoval, S.; Camps, E.; Castrejón-Sánchez, V.H.; Campos-González, E.; Zapata-Torres, M.; Pérez-Centeno, A.; Santana-Aranda, M.A. Physical properties of a non-transparent cadmium oxide thick film deposited at low fluence by pulsed laser deposition. *Mat. Res. Bull.* **2016**, *76*, 376–383. [\[CrossRef\]](#)
13. Quiñones-Galván, J.G.; Camps, E.; Campos-González, E.; Hernández-Hernández, A.; Santana-Aranda, M.A.; Pérez-Centeno, A.; Guillén-Cervantes, A.; Santoyo-Salazar, J.; Zelaya-Angel, O.; de Moure-Flores, F. Influence of plasma parameters and substrate temperature on the structural and optical properties of CdTe thin films deposited on glass by laser ablation. *J. Appl. Phys.* **2015**, *118*, 125304. [\[CrossRef\]](#)
14. Le, P.H.; Liao, C.-N.; Luo, C.W.; Leu, J. Thermoelectric properties of nanostructured bismuth–telluride thin films grown using pulsed laser deposition. *J. Alloys Compd.* **2014**, *615*, 546. [\[CrossRef\]](#)
15. Dauscher, A.; Thomy, A.; Scherrer, H. Pulsed laser deposition of Bi_2Te_3 thin films. *Thin Solid Films* **1996**, *280*, 61–66. [\[CrossRef\]](#)
16. Faraji, L.S.; Singh, R.P.; Allahkarami, M. Pulsed laser deposition of bismuth telluride thin film and annealing effects. *Eur. Phys. J. Appl. Phys.* **2009**, *46*, 20501. [\[CrossRef\]](#)
17. Raghuvver, S.; Makala, K.; Jagannadham, B.C. Sales, Pulsed laser deposition of Bi_2Te_3 -based thermoelectric thin films. *J. App. Phys.* **2003**, *94*, 3907.
18. Shupenev, A.E.; Korshunov, I.S.; Grigoryants, A.G. On the Pulsed-Laser Deposition of Bismuth-Telluride Thin Films on Polyimide Substrates. *Semiconductors* **2020**, *54*, 378–382. [\[CrossRef\]](#)
19. Tuyen, L.T.C.; Le, P.H.; Jian, S.-R. Nanostructuring Bi_2Te_3 -Based Thermoelectric Thin-Films Grown Using Pulsed Laser Deposition. In *Materials at the Nanoscale*; Awadesh Kumar Mallik; IntechOpen Limited: London, UK, 2021.
20. Quiñones-Galván, J.G.; Camps, E.; Muhl, S.; Flores, M.; Campos-González, E. Influence of plasma density on the chemical composition and structural properties of pulsed laser deposited TiAlN thin films. *Phys. Plasmas* **2014**, *21*, 053509. [\[CrossRef\]](#)

21. Guerrero de León, J.A.; Quiñones-Galván, J.G.; Pérez-Centeno, A.; Gómez-Rosas, G.; Camps, E.; Santana-Aranda, M.A. Effect of the Cu plasma density on ZnO:Cu thin films grown by PLD. *Mater. Res. Express* **2018**, *5*, 066417. [\[CrossRef\]](#)
22. Saracho-González, S.; Pérez-Centeno, A.; Santana-Aranda, M.A.; Gómez-Rosas, G.; Chávez-Chávez, A.; Camps, E.; Rivera, L.P.; de Moure-Flores, F.; Zelaya-Angel, O.; Quiñones-Galván, J.G. Effect of the combination of Cu and CdTe plasmas on the structural and optical properties of CdTe:Cu thin films deposited by laser ablation. *Mat. Sci. Semicond. Proc.* **2018**, *87*, 7–12. [\[CrossRef\]](#)
23. Rivera, L.P.; García, E.; Cardona, D.; Pérez-Centeno, A.; Camps, E.; Santana-Aranda, M.A.; Gómez-Rosas, G.; de Moure-Flores, F.; Chávez-Chávez, A.; Quiñones-Galván, J.G. CdTe:Sn thin films deposited by the simultaneous laser ablation of CdTe and Sn targets. *Mater. Res. Express* **2020**, *7*, 015905. [\[CrossRef\]](#)
24. Quiñones-Galván, J.G.; Cardona, D.; Rivera, L.P.; Gómez-Rosas, G.; Chávez-Chávez, A. Effect of the copper plasma density on the growth of SiO_x-Cu thin films by PLD. *Mat. Lett.* **2021**, *284*, 129024. [\[CrossRef\]](#)
25. Bulgakova, N.M.; Bulgakov, A.V.; Bobrenok, O.F. Double layer effects in laser-ablation plasma plumes. *Phys. Rev. E* **2000**, *62*, 5624–5635. [\[CrossRef\]](#) [\[PubMed\]](#)
26. Doggett, B.; Lunney, J.G. Langmuir probe characterization of laser ablation plasmas. *J. Appl. Phys.* **2009**, *105*, 033306. [\[CrossRef\]](#)
27. van de Riet, E.; Nillesen, C.J.C.M.; Dieleman, J. Reduction of droplet emission and target roughening in laser ablation and deposition of metals. *J. Appl. Phys.* **1993**, *74*, 2008–2012. [\[CrossRef\]](#)
28. Völklein, F.; Baier, V.; Dillner, U.; Kessler, E. Transport properties of flash-evaporated (Bi_{1-x}Sb_x)₂Te₃ films I: Optimization of film properties. *Thin Solid Films* **1990**, *187*, 253–262. [\[CrossRef\]](#)
29. Cao, R.; Zhu, Z.; Li, X.-J.; Hu, X.; Song, H. Enhanced thermoelectric properties of the Lu-doped and CNT-dispersed Bi₂Te₃ alloy. *Appl. Phys. A* **2019**, *125*, 126. [\[CrossRef\]](#)
30. Li, S.; Zhang, S.; He, Z.; Toprak, M.; Stiewe, C.; Muhammed, M.; Müller, E. Novel Solution Route Synthesis of Low Thermal Conductivity Nanocrystalline Bismuth Telluride. *J. Nanosci. Nanotechnol.* **2010**, *10*, 7658–7662. [\[CrossRef\]](#)
31. Takashiri, M.; Tanaka, S.; Miyazaki, K.; Tsukamoto, H. Thermoelectric properties of n-type nanocrystalline bismuth-telluride-based thin films deposited by flash evaporation. *J. Appl. Phys.* **2007**, *101*, 074301. [\[CrossRef\]](#)
32. Yoon, S.; Kwon, O.-J.; Ahn, S.; Kim, J.-Y.; Koo, H.; Bae, S.-H.; Cho, J.-Y.; Kim, J.-S.; Park, C. The Effect of Grain Size and Density on the Thermoelectric Properties of Bi₂Te₃-PbTe Compounds. *J. Electron. Mater.* **2013**, *42*, 3390–3396. [\[CrossRef\]](#)
33. Bellucci, A.; Mastellone, M.; Girolami, M.; Orlando, S.; Medici, L.; Mezzi, A.; Kaciulis, S.; Polini, R.; Trucchi, D.M. ZnSb-based thin films prepared by ns-PLD for thermoelectric applications. *App. Surf. Sci.* **2017**, *418*, 589–593. [\[CrossRef\]](#)
34. Richter, W.; Becker, C.R. A Raman and far-infrared investigation of phonons in the rhombohedral V2–VI3 compounds Bi₂Te₃, Bi₂Se₃, Sb₂Te₃ and Bi₂(Te_{1-x}Se_x)₃. *Phys. Status Solidi B* **1977**, *84*, 619–628. [\[CrossRef\]](#)
35. Russo, V.; Bailini, A.; Zamboni, M.; Passoni, M.; Conti, C.; Casari, C.S.; Bassi, A.L.; Bottani, C.E. Raman spectroscopy of Bi-Te thin films. *J. Raman Spectrosc.* **2008**, *39*, 205–210. [\[CrossRef\]](#)
36. Goncalves, L.M.; Couto, C.; Alpuim, P.; Rolo, A.G.; Völklein, F.; Correia, J.H. Optimization of thermoelectric properties on Bi₂Te₃ thin films deposited by thermal co-evaporation. *Thin Solid Films* **2010**, *518*, 2816–2821. [\[CrossRef\]](#)
37. Shahil, K.M.F.; Hossain, M.Z.; Goyal, V.; Balandin, A.A. Micro-Raman spectroscopy of mechanically exfoliated few-quintuple layers of Bi₂Te₃, Bi₂Se₃, and Sb₂Te₃ materials. *J. Appl. Phys.* **2012**, *111*, 054305. [\[CrossRef\]](#)
38. Bando, H.; Koizumi, K.; Oikawa, Y.; Daikohara, K.; Kulbachinskii, V.A.; Ozaki, H. The time-dependent process of oxidation of the surface of Bi₂Te₃ studied by X-ray photoelectron spectroscopy. *J. Phys. Condens. Matter* **2000**, *12*, 5607–5616. [\[CrossRef\]](#)
39. Bahl, M.K.; Watson, R.L.; Irgolic, K.J. X-ray photoemission studies of tellurium and some of its compounds. *Chem. Phys.* **1977**, *66*, 5526–5535. [\[CrossRef\]](#)
40. Ahmad, M.; Agarwal, K.; Mehta, B.R. An anomalously high Seebeck coefficient and power factor in ultrathin Bi₂Te₃ film: Spin-orbit interaction. *J. Appl. Phys.* **2020**, *128*, 035108. [\[CrossRef\]](#)

Disclaimer/Publisher’s Note: The statements, opinions and data contained in all publications are solely those of the individual author(s) and contributor(s) and not of MDPI and/or the editor(s). MDPI and/or the editor(s) disclaim responsibility for any injury to people or property resulting from any ideas, methods, instructions or products referred to in the content.